Article

Evaluation of Photodynamic Therapy as a New Therapeutic Approach Using Quinizarin-Loaded Nanocapsules: In Vitro Cytotoxicity, Permeation in 3D Bioprinted Skin Equivalent and In Vitro Cytokines Modulation

Stéphanie Rochetti do Amaral , Camila Fernanda Amantino , Aleksandar Atanasov , Stefanie Souza , Richard Moakes , Sonia M Oliani , Liam M Grover , Fernando Lucas Primo *

Posted Date: 21 May 2024

doi: 10.20944/preprints202405.1323.v1

Keywords: Drug Delivery; Nanotechnology; Skin Inflammation; Photodynamics

 doi:10.20944/preprints202405.1323.v1

Article

Evaluation of Photodynamic Therapy as a New Therapeutic Approach Using Quinizarin-Loaded Nanocapsules: *In Vitro* Cytotoxicity, Permeation in 3D Bioprinted Skin Equivalent and *In Vitro* Cytokines Modulation

Stéphanie R. do Amaral [1], Camila F. Amantino [2], Aleksandar Atanasov [3], Stefanie Souza [4], Richard Moakes [3], Sônia M. Oliani [4], Liam M. Grover [3] and Fernando L. Primo [1,*]

[1] School of Pharmaceutical Sciences - Department of Bioprocess and Biotechnology Engineering, São Paulo State University (UNESP), Araraquara 14800-903, SP, Brazil.
[2] São Paulo Federal Institute of Education, Science and Technology (IFSP), Matão 15991-502, SP, Brazil.
[3] School of Chemical Engineering, University of Birmingham, Birmingham B15 2TT, United Kingdom.
[4] Department of Biology, Institute of Biosciences, Humanities and Exact Sciences (IBILCE), São Paulo State University (UNESP), São José do Rio Preto 15054-000, SP, Brazil.
* Correspondence: fenando.primo@unesp.br.

Abstract: Skin inflammation associated with chronic diseases has the direct action of keratinocytes in its immunopathogenesis, leading to a series of immune responses. However, there are still no highly targeted treatments, and the development of more specific therapies is highly desirable. In the present work, nanocapsules containing quinizarin (QZ/NC) were developed, evaluating their act in a model of the keratinocytes inflammatory process *in vitro* with the action of Photodynamic Therapy, analyzing the permeation in a 3D skin model. Physicochemical, stability, cytotoxicity and permeation analyses of the nanomaterials were carried out. The nanocapsules showed desirable physicochemical characteristics and were stable during the analysis period, without spectroscopic modifications. The cell viability test carried out showed no cytotoxicity at the lowest QZ/NC concentrations. The permeation and cellular uptake studies showed the permeation of QZ/NC in 3D skin models and the intracellular incorporation and internalization of the drug, enhancing its action in the drug delivery technique. Promising results were presented using the model developed to induce the inflammatory process *in vitro* and applying the synthesized nanomaterial in conjunction with PDT, where a decrease in the levels of cytokines analyzed was observed, representing a possible new therapeutic approach for inflammatory skin diseases.

Keywords: nanotechnology; photodynamics; skin inflammation

1. Introduction

The skin is the largest organ in the human body. It performs vital protective functions and has three layers: the epidermis, dermis and the subcutaneous tissue. The epidermis is the outermost layer and is mainly made up of keratinocytes (95%), as well as cells such as melanocytes, Langerhans cells and Merkel cells. Keratinocytes are fundamental cells in the skin's inflammatory process and related immune responses, interacting with immune system cells by releasing cytokines and chemokines [1–3].

Epithelial cells are influenced by intrinsic genetic factors, as well as by the environment and the microbiome, which can have a direct influence on immune responses to potential allergens and pathogens. During an inflammatory response, keratinocytes release pro-inflammatory cytokines (TNF-α, IL-1α, IL-1β and IL-18. IL-1), inducing the expression of new inflammatory cytokines (IL-6, IL-8 and TNF-α) and adhesion molecules on endothelial cells, leading to the targeting of effector T

 doi:10.20944/preprints202405.1323.v1

cells to the site of inflammation, and each type of injury/inflammation leads to different activation and recruitment of the most convenient cell subset. Uncontrolled immune responses can lead to chronic inflammatory diseases such as psoriasis and atopic dermatitis [4,5].

Psoriasis, atopic dermatitis and rosacea are the most common chronic skin diseases, characterized by hyperproliferation of keratinocytes, involving multifactorial inflammatory responses linked to highly complex autoimmune responses [6,7]. Psoriasis it´s characterized by excessive growth and abnormal differentiation of keratinocytes leading to skin lesions, resulting from inflammatory and angiogenic stimuli, linked to increased expression of immune cells and inflammatory cytokines. Currently 2-4% of the world's population is affected, giving anti-psoriatic drugs a market worth close to 18.8 billion USD in 2021 [8–10]. The inflammatory mechanism of psoriasis involves the presence of keratinocytes, leukocytes, T cells, macrophages, neutrophils, mast cells, dendritic, followed by the release of inflammatory cytokines [11]. Keratinocytes are activated by pro-inflammatory cytokines such as TNF-α and IL-1, which are elevated in psoriatic lesions. Once activated, keratinocytes change their proliferation and differentiation, thickening the epidermis and leading to increased production of chemokines, leading to a positive feedback loop between keratinocytes and immune system cells [12].

Considering psoriasis treatment, the biggest obstacle is the physiology of the skin, which becomes stiffer and more impermeable to medicines, limiting their bioavailability at the lower epidermis [10]. The first line of treatment for psoriasis and others chronic skin diseases, consists of topical therapy. If this treatment is no longer effective, it is proceeded with phototherapy and systemic drug administration [9]. However, these methods are associated with numerous side effects, such as nausea, irritation of the skin, hepatotoxicity, in addition to drug resistance. Combined, these factors define the need for more effective treatments, with greater drug targeting and bioavailability [13,14].

Photodynamic Therapy (PDT) is a widely used therapeutic modality, with promising results in patients with various types of superficial skin diseases such as psoriasis [15]. Contrary to biological agents and other medications, PDT is a powerful and secure technique with no systemic side effects [16]. The mechanism of action of PDT is based on photochemistry-controlled reactions, which can induce changes in the cellular metabolism, including induction of cell death via apoptosis and/or necrosis based on the cell type, light intensity, and PS type [9,17,18]. One of the biggest challenges of PDT is the choice of the most suitable photosensitizer, which essential characteristics such as biological affinity, biodistribution and minimum photodynamic potential for application [15]. Quinizarin, (QZ) (1,4 dihydroxyanthraquinone), an anthraquinone derivative compound, shows secondary biological activities characteristics as anti-inflammatory, antioxidant, antibacterial action [19–21], and high potential as photosensitizing compounds [22] showing high-density planar and quinoid conjugated aromatic groups electronics, which may contribute to the generation of reactive oxygen species (ROS), [23–26], with a high potential as photosensitizing compounds from a PDT perspective [22].

However, there are some limitations to the use of Anthraquinones in PDT, as their low solubility in aqueous media, which can cause lack of selectivity in the treatment. Pharmaceutical nanotechnology is a valuable resource, which can significantly influence the use of anthraquinone derivatives in PDT, increasing their permeation at the required site, as well as their controlled and sustained release [27]. Among the main colloidal nanocarriers with potential application, the polymeric and emulsified systems come in focus, especially polymeric nanocapsules (NC). They are mostly composed of biodegradable polymers, biocompatible, avoiding toxicity, and presenting high efficiency of encapsulation [28]. In addition, the polymeric wrapping present in nanocapsules preserves the drug from the degradative effects of factors such as light, oxygen, and the acidic stomach environment, and controls the release of the internalized active into the biological targets of interest [29].

The development of new therapies has been underpinned for years by two-dimensional culture (monolayer) or animal models, but limitations linked to reliability and reproducibility still exist. The concept of Tissue Engineering has evolved rapidly in this context, opening space for three-dimensional printing, an automated and highly efficient technology for creating porous and complex structures, capable of reliable systems for drug testing and disease modeling [30]. Technologies, such as the Suspended layer additive manufacture (SLAM) method, aim to overcome the limitations of 3D

 doi:10.20944/preprints202405.1323.v1

bioprinting cell-laden constructs. The technology presents a solution for creating hydrogels with defined properties, making it a valuable tool for recapitulating in vivo interactions, mimicking the complexity of real tissues [31–33].

The present study proposes the development and characterization of a 2D model of inflammatory process in human keratinocyte cells for the application of Photodynamic Therapy using polymeric quinizarin-loaded nanocapsules, an anthraquinone derivative with secondary biological activities, evaluating the joint action of nanotechnology and PDT in a new therapeutic modality, combined with Tissue Engineering.

2. Materials and Methods

2.1. Development of Polymeric Nanoparticles Loaded with Quinizarin

Polymeric NCs (QZ/NC) were prepared using the nanoprecipitation method as described by Mora-Huertas et al. [24] with modifications by Siqueira-Moura et al. [34], at the concentration of 0.1 $mg.mL^{-1}$ Quinizarin. The coating co-polymer poly (L-lactic acid-co-glycolic acid) - PLGA 50:50 (0.75% w/v) and lecithin (high purity soy phosphatidylcholine) at 1.75% m/v were dissolved in 15 mL of acetone at 40 °C (characterizing the organic phase) and slowly added by dripping at the rate of 1.0 $g.s^{-1}$, under the aqueous solution, containing Pluronic F-68 (1.25% m/v) in 30 mL of water under moderate and constant stirring (250 rpm) at 40°C. The emulsification and interfacial coating process was started after phase mixing directly in a 250 mL jacketed reactor coupled to a thermostatic bath under constant circulation. Subsequently, the organic solvent was removed to finalize the nanoemulsification process, through the route-evaporation step at 40 °C and 225 rpm rotation under reduced pressure, obtaining a final formulation volume of 10 mL.

2.2. Characterization of Particle Size, Polydispersity Index (PdI) and Zeta Potential

The physicochemical analyses were performed following the standard operating procedures of the equipment Zetasizer™, model Nano ZS90 Malvern, obtaining parameters of Particle Size, Polydispersity Index (PdI) and Zeta Potential.

2.3. Atomic Force Microscopy

Atomic force microscopy allows the topographical surface of nanomaterials to be analyzed. Images of the QZ/NC were taken at room temperature using a Shimadzu Scanning Probe Microscope model SPM-9600. The sample was prepared on a mica surface, where a drop (5.0 µL) of the formulation was deposited. The images were obtained using the intermittent contact method, with a 124 µm long cantilever, operating at a resonance frequency in the range of 324-369 KHz, rigidity of 34-51 N/m and constant force.

2.4. 3D Fluorescence Emission Spectroscopy UV/Vis

The 3D fluorescence emission spectra of QZ in acetonitrile and after nanoencapsulation (QZ/NC) were obtained as part of the spectroscopic characterization. Analyses were carried out using a fluorimeter (Shimadzu model RF-6000) with the following parameters: emission wavelength (525 - 685nm); excitation wavelength (400 - 520nm); data interval: 2nm; excitation band: 1.5nm and emission band 3nm.

2.5. Cell Culture

The dermal fibroblast (HDFs – ATCC™ PCS-201-010™), adipose-derived stem cells (ADSCs – Thermo Fisher Scientific R7788115), human epidermal keratinocytes (NHEKs - Thermo Fisher Scientific C0015C), Immortalized human keratinocyte (HaCaT- Cell line service) and commercial murine fibroblast (NIH/3T3 - ATCC™ CRL-1658™) cell lines were cultivated using the standard cultivation protocol. The cell lines were cultured in an incubator with 5% CO_2 at 37 °C, and the culture was conducted until the confluence stage was reached, where the cells were used for the subsequent assays.

2.6. Cellular Uptake

 doi:10.20944/preprints202405.1323.v1

Immortalized human keratinocyte lineage cells (HaCaT - cell line service) were plated in 24-well plates ($3x10^4$ cells.well^{-1}) and maintained at 37 °C in an atmosphere containing 5% CO_2 for 24h. Subsequently, QZ/NC were placed at a concentration of 15 μg.mL^{-1} at three different times (3h, 6h and 24) in order to analyze the best time for cell internalization. After the mentioned times, the respective plates were quantified using the EnSpireTM microplate reader (PerkinElmer, USA) where the fluorescence intensity was analyzed.

2.7. Cytotoxicity Assay Using Resazurin Test

NIH/3T3 and HaCaT cells were seeded into a 96-wells plate (5×10^3 cells.well^{-1}), after 24 h was added free QZ and QZ/NC in range concentration of 2.5–70 μg.mL^{-1} using mean DMEM for dilutions and incubated for 3 h for NIH/3T3 and 24h for HaCaT as suggested by ISO 10993-5. After 24 h of treatment, 20 μL of Resazurin solution (25 μg.mL^{-1} in PBS) and 180 mL of DMEM were added and incubated for 4 h. Afterwards the wells analyses were carried out in the microplate reader EnSpire™ (PerkinElmer, USA) in 570 nm and the basal absorbance was corrected in 590 nm. The percentage of viable cells was calculated following the Eq. (1).

$$\text{Viable cells (\%)} = (\text{O.D.sample/O.D.control}) \times 100 \quad (1)$$

2.8. Permeation Study in a New 3D Bioprinted Skin Equivalent: Suspended layer Additive Manufacturing (SLAM) Method

The 3D skin equivalents, and the printing media were prepared as described by Moakes et al [33] following the method of suspended layer additive manufacturing. The layers were prepared from a blend of collagen to pectin: papillary layer (2:1 blend containing $3x10^6$ cells.mL^{-1} (HDFs—passage 8); reticular layer (2:1 blend containing $1.5x10^6$ cells.mL^{-1} (HDFs—passage 7) and 1:1 blend containing $5x10^5$ cells.mL^{-1} (ADCSs—passage 3). The construct's G-code was sent to the printing program to print a tri-layer with the following dimensions with a cylindrical shape: A=225mm^2; H=1.2mm in a 0.5% w/v Agarose fluid gel support bath. Subsequently, the constructs were gelled through the addition of a 200 mmol.L^{-1} $CaCl_{2(aq)}$ solution to the support bath, followed by a 30-min incubation at 37°C. The constructs were then transferred into clean wells for culture at 37 °C and 5% CO_2 with supplemented DMEM medium (10% v/v Fetal Bovine Serum, 1% v/v PenStrep; Sigma-Aldrich, UK) for 14 days. Keratinocyte cells (NHEKs $2.5x10^5$ cells.mL^{-1} — passage 4**)** were placed on top of the constructs and cultured for another 7 days, forming the epidermal layer. The QZ/NC, at a concentration of 15μg.mL^{-1}, defined as the safety limit, and free QZ (15μg.mL^{-1}), both suspended in DMEM, were added to the top of the equivalents (80μL), inside a cylindrical support, which ensured that the sample would be concentrated at the top of the construct; a control was also prepared with DMEM only. After 24 hours, cross-sections were made and the samples were analyzed using a SPARK microplate reader (TECAN, SWI) and a Cytation imaging reader (BioTek, USA) where the fluorescence intensity was observed.

2.9. Induction of Inflammatory Process in HaCaT Cells and Application of Photodynamic Therapy

HaCaT cells were used as a biological model for the development of the inflammatory model. The cells were cultured as described in 2.7 and plated in 24-well plates. The cells were induced with bacterial lipopolysaccharide (LPS) at a concentration of 10 μg.mL^{-1} and incubated for 24h - 37°C, 5% CO_2. After the mentioned period, QZ/NC was added at the concentration of 15 μg.mL^{-1}. Subsequently, the cells still with LPS and QZ/NC were submitted to PDT, where a 24-well LED tabletop photoactivation system (IrradLED/Biopdi) emitting at 470 nm with 37.2 mW optical power was used. The energy densities (fluences) used were: 1.0 J.cm^{-2} (D1), 5.0 J.cm^{-2} (D2) and 10 J.cm^{-2} (D3) for the respective exposure times: 27s, 134s and 269s. Two plates were made for post-irradiation analysis.

2.10. Enzyme-Linked Immunosorbent Assay (ELISA)

For in vitro assays, IL-1β, IL-8 and MCP-1 levels of cell supernatants were detected using the commercially available human quantikine ELISA kit (BD Biosciences, California, USA), and according to the manufacturer's instructions, following the protocol previously described by Cardoso et al. [35]. Briefly, 100 μL of each of the standards, controls, and samples were loaded into 96-well polystyrene microplates wells, containing 100 μL of assay diluent in triplicate. After incubation for 2h, the microplates were washed 4 times. Then, 200 μL of specific conjugate solutions were added to

 doi:10.20944/preprints202405.1323.v1

each well for 2h, washed, and 200 µL of a substrate solution was added. After 20 min of incubation, 50 µL of the stop solution stop solution was added and the optical density was read at 450 nm using a microplate reader microplate reader (Molecular Devices, Sunnyvale, CA) with a correction wavelength of 540 nm.

2.11. Statistical Analysis

Statistical analysis was performed using one-way analysis of variance (one-way ANOVA), with Tukey's test (Cytotoxicity) and Dunnett 's test (ELISA) as post-test for multiple comparisons analysis between the groups (*p<0,05; **p<0,001).

3. Results and Discussion

3.1. Physical-Chemical and Two-Dimensional Topography Analysis: Particle Size, PdI, Zeta Potential and AFM

Stability studies are essential for pharmaceutical and industrial application of nanomaterials [36]. The particle size, polydispersity index (PdI) and Zeta potential (ζ), which provides surface charge, were determined using the Dynamic Light Scattering (DLS) technique. The average of the particle number values obtained for QZ/NC and for Unloaded/NC were expressed as mean ± standard deviation and are shown in Table 1.

Table 1. Data of average* Particle Size, PdI, and Zeta Potential of QZ/NC and Unloaded/NC.

Nanomaterial	Average Particle Size (nm)	PdI	Zeta Potential (mV)
QZ/NC	103.9 ± 34.5	0.4 ± 0.03	-31.8 ± 0.723
Unloaded/NC	137.2 ± 46.1	0.5 ± 0.06	-35.1 ± 1.107

*n=3.

Both synthesized nanomaterials (QZ/NC and Unloaded/NC) showed a satisfactory profile, which is expected for colloidal systems submicron polymers. The PdI values for show a polydispersion of the systems, indicating possible agglomeration and/or variation in particle size. However, the percentages of number of particles (97.9 %) in the region of the predominant average size, indicate a monodisperse system with variation relative to the larger particle distribution. The zeta potential values remained within the proposed stability range within the analysis period (+30mV, -30mV). Within the 61-day post-synthesis period, QZ/NC and Empty/QZ remained stable within the analyzed parameters, as can be seen in Figure 1-A. The determination of physicochemical parameters is extremely important, describing the nanomaterial and evaluating its behavior when inserted in a biological environment. Particle size, polydispersity index, and Zeta potential are fundamental analyses that describe nanoparticles. The surface characteristics, indicated by the Zeta potential, influence the biological performance and safety of the nanomaterial, determining its biodistribution and special stability and, consequently, indicating the drug release in biological targets [37]. These parameters, associated with the polydispersity index (PdI) indicate the stability of nanomaterials that are designed from better performance compared to macromaterials applied in biological use. Characteristics such as particle size are essential for the development of effective nanomaterials for topical application, considering the cutaneous permeation, where particles with submicron size tend to penetrate in a facilitated manner through the skin, reaching the systemic circulation [38,39].

The AFM analysis of the QZ/NC, shown in Figure 1 - B, shows clear images of particles with a well-defined spherical shape, with a size within the expected, with an average around 65nm, since previous DLS analyses, indicating that the particles analyzed previously had a larger particle size than the MFA analysis, which is because DLS measures the particle's hydrodynamic radius or solvation radius. Thus, the analysis confirms the average particle size expected for nanostructured polymeric systems and shows the characteristic spherical morphology of the system developed, with excellent correlation with the hydrodynamic sizes obtained by the DLS technique, where the QZ/NC show no deformations on the surface, indicating a homogeneous particle formed only by the PLGA, which covers the nanocapsules [27].

 doi:10.20944/preprints202405.1323.v1

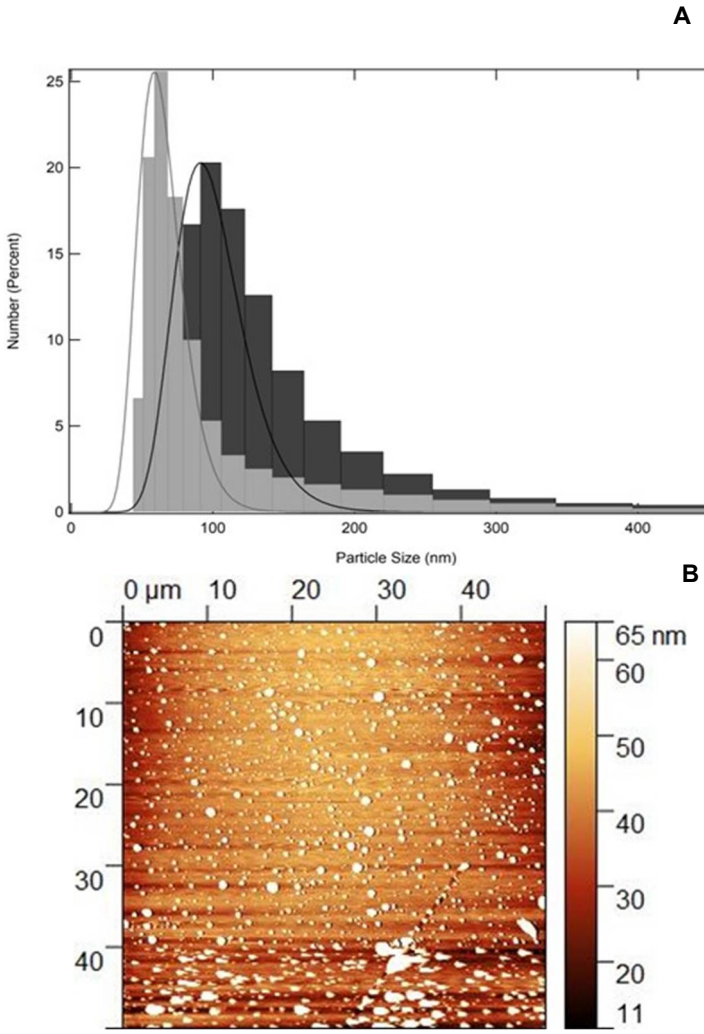

Figure 1. A: Size distribution profile of the developed NC using dynamic light scattering technique. Unloaded/NC (gray) and QZ/NC (black) at 61 days after synthesis. **B:** Two-dimensional photomicrograph of QZ/NC obtained using the AFM technique.

3.2. 3D Fluorescence Emission Spectroscopy UV/Vis

The 3D fluorescence emission spectra profiles of free QZ and QZ/NC were obtained by UV/Vis fluorescence emission spectroscopy studies, as shown in Figure 2. The fluorescence intensity maximum profile was obtained at 569 nm from the excitation at 480 nm.

 doi:10.20944/preprints202405.1323.v1

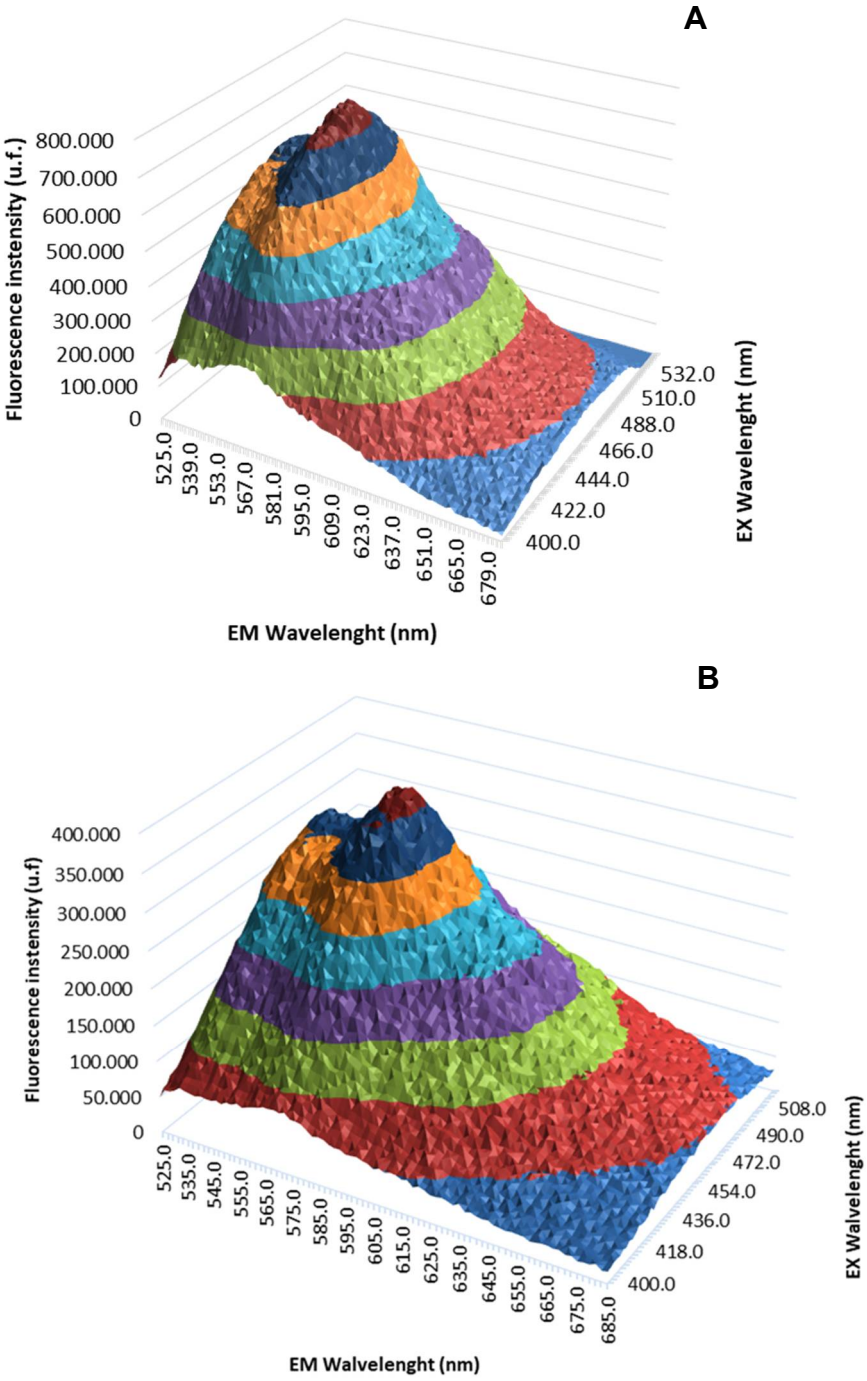

Figure 2. 3D fluorescence spectra of free Quinizarin (A) and Quinizarin nanoencapsulated (B).

The analysis of compounds is of fundamental, facilitating their characterization and the identification of possible modifications. The fluorescence method, when compared to other spectral methods, has shown significant advantages, due to its simplicity, speed, high sensitivity, with emphasis on 3D fluorescence spectroscopy, which measures emission spectra over a range of excitation wavelengths, allowing a more extensive identification of samples, becoming a powerful tool in the classification and identification of substances [40,41].

There were no significant changes in fluorescence profile of free QZ when nanoencapsulated, with no reaction of the active with the components used to prepare the nanostructured system, promoting support for the use of QZ/NC in future biological tests. Previous studies carried out with quinizarin in a spray dryer nanosystem have shown favorable results and in agreement with the one presented. In particular, no changes were observed in the molecule's profile after encapsulation, with

 doi:10.20944/preprints202405.1323.v1

a high association rate (72.3%), which is satisfactory for subsequent in vitro studies [42]. Considering the application in Photodynamic Therapy, maintaining the photophysical properties of the PS in the ground state is extremely important, ensuring absorption in the visible region of the electromagnetic spectrum at the optimal excitation wavelength.

3.3. Cytotoxicity Assay Using Resazurin Test – NIH/3T3 Cells

NIH/3T3 cells were used as preliminary assays to analyze the cytotoxicity of the material. QZ/NC was analyzed at concentrations of 2.5 - 70μg.mL^{-1}, Unloaded/QZ 50% (v/v) and free QZ (50 and 70 μg.mL^{-1}). These data are interesting and are in accordance with the incubation times suggested in the international standard ISO 10993-5 for cytotoxicity testing of nanomaterials.

Cytotoxicity studies are extremely important and necessary in drug development and synthesis of new medicines for assessing the in vitro biological compatibility profile of active ingredients and compounds with potential for biological application. There are also tests that help determine important nanotechnology development parameters, such as IC10 and IC50, which are exactly the inhibitory concentrations that induce a 10% and 50% reduction in cell viability respectively.

Table 2. Cellular viability[§] obtained from in vitro cytotoxicity assay of QZ/NC, Unloaded/NC and free QZ on murine fibroblast cell lines NIH/3T3 (ATCC® CRL-1658) at concentrations of 2.5; 5; 15; 25; 50; 70 μg.mL^{-1} (QZ/NC), 50% (v/v) NC/empty and free QZ at concentrations of 50 and 70 μg.mL^{-1}. Statistical significance was determined using the One-way ANOVA test of analysis of variance at 95% significance level, followed by Tukey post-test for multiple comparisons (*p<0.05, **p<0.001).

Sample/Concentration (μg.mL^{-1})	3T3 - Cellular Viability (%)	Significance level (*p<0.05, **p<0.001)
Control	**100**	**-**
Unloaded Nanocapsule	**81.43**	**-**
Free Quinizarin 50	**100.06**	**-**
Free Quinizarin 70	**91.30**	**-**
QZ/NC 2.5	**98.32**	**-**
QZ/NC 5.0	**100.92**	**-**
QZ/NC 15.0	**96.69**	**-**
QZ/NC 25.0	**69.82**	*
QZ/NC 50	**9.66**	**
QZ/NC 70	**9.02**	**

[§]*n=3.*

As evidenced in Table 2, the absence of cytotoxicity was observed at the lower concentrations of QZ/NC, Unloaded/NC, and free QZ at both concentrations tested. At the higher concentrations of QZ/NC there was a decrease in cell viability, of approximately 30% (25 μg.mL^{-1}) and 90% (50 and 70 μg.mL^{-1}). The concentration of 15 μg.mL^{-1} was chosen for the development of the sequential investigative biological assays, considered the in vitro safety threshold

3.4. Cell Internalization and Permeation Study

The processes of cell permeation and internalization are influenced by several variables, such as the size of the nanomaterial chosen, as the concentration, pharmaceutical form, surface characteristics and the internal structure [43]. The greatest limitations involved in the development of drugs for topical and transdermal application is the permeation barrier provided by the stratum corneum of the skin, composed of rigid layers rich in keratin and lipid intercellular matrix, which directly influences the therapeutic result [44,45].

In order to determine the internalization of QZ/NC in HaCaT cells, three different incubation times (3, 6 and 24 hours) were analyzed QZ/NC at the concentration of 15 μg.mL^{-1}. Higher internalization was observed for QZ/NC when compared to free QZ (Figure 3), demonstrating the desired effect of increased cytoplasmic internalization of the nanocarrier active.

Another data obtained in the assay was the best incubation time relative to the best internalization rates of the active. According to the following results, the time of 24h presented a fluorescence intensity of QZ much higher than the previous times, indicating an internalization 9x

 doi:10.20944/preprints202405.1323.v1

higher than the others. These data are in accordance with the incubation times suggested in the international standard ISO 10993-5 for cytotoxicity testing of nanomaterials.

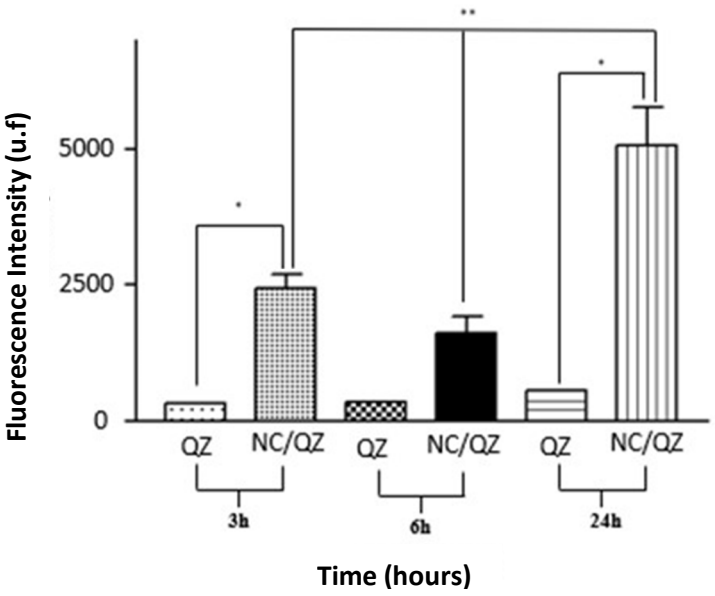

Figure 3. Cellular uptake study in HaCaT cells at a concentration of 15 µg.mL^{-1} evaluating the cellular internalization of free Quinizarin (QZ) and nanoencapsulated form (QZ/NC) at 3, 6 and 24 hours. Statistical significance was determined using the One-way ANOVA test of variance, with 95% significance level, followed by Tukey post-test for multiple comparisons, where *statistical difference obtained between free QZ and QZ/NC, **statistical difference obtained between QZ/NC in the three tested times ($p<0.05$).

The permeation of QZ/NC and free quinizarin was evaluated using a 3D bioprinted skin equivalent as a model, developed by the suspended layer additive manufacturing (SLAM) method, where computer-aided design (CAD) was used to create the design of the three layers, mimicking the skin. The composition of the bioink consisted of a mixture of pectin, which is similar to the polysaccharides found in native ECM, and collagen, mimicking the composition of skin [33]. Analyses were conducted to assess permeation after 24 hours in cross-sections, evaluating permeation throughout the model (from top to bottom), using the previously determined excitation and fluorescence emission parameters of quinizarin. The concentration used was 15µg/mL, defined in the cytotoxicity experiment as the drug's safety threshold.

The fluorescence analyses, shown in Figure 4, showed permeation of QZ/NC in all the layers of the three-dimensional model. Observed were fluorescence signals characteristic of the QZ/NC, which is one of the main desired effects and justifies the use of nanotechnology for biological applications Quantitative assessment of the fluorescent signals showed no statistically significant difference between the control (DMEM) and the free QZ, suggesting impaired permeability of free QZ through the skin model barrier. Conversely, the QZ/NC samples exhibited a statistically significant ($*p<0.05$) 1.25x increase in the fluorescent signal. Previous studies analyzing the permeation of nanoparticles in human cadaver skin have observed an increase and improvement in the permeation of nanostructured compounds [44]. Also, considering the structure of the skin in inflammatory diseases such as psoriasis, where the hyperproliferation of keratinocytes and the inflammatory process make the skin rigid and impermeable, the use of polymeric nanoparticles is highly applicable, since they promote greater bioavailability and permeability in the stratum corneum of the skin [10].

 doi:10.20944/preprints202405.1323.v1

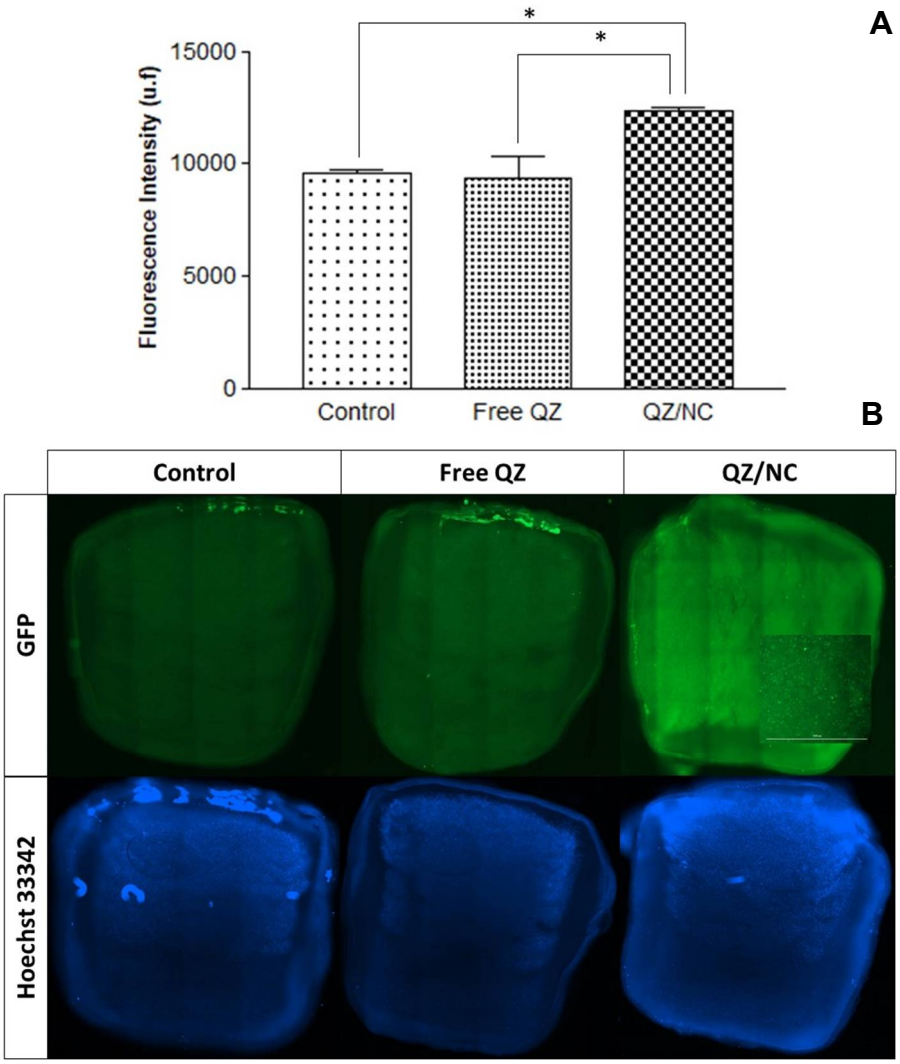

Figure 4. Analysis of permeation in the three-dimensional skin model by evaluating fluorescence intensity (A) and cross-sectional images (B) using a SPARK microplate reader (TECAN, SWI) and an Cytation imagin reader (BioTek, USA) respectively. The control, containing only DMEM, free quinizarin and QZ/NC were analyzed. Statistical significance was determined using the analysis of variance test One-way ANOVA, at 95% significance level, followed by Tukey post-test for multiple comparisons (*p<0,05).

3.5. Cytotoxicity Assay Using Resazurin Test – HaCaT Cells

The modulation of the human epidermis through the use of monolayer keratinocytes has been studied extensively, making it possible to understand the functional characteristics of interactions within the cell [46]. An additional cell viability test was carried out on human keratinocyte cells (HaCaT), assessing the toxicity of QZ/NC at different concentrations (2.5 - 50 $\mu g.mL^{-1}$), since the keratinocyte lineage was used to modulate the inflammatory process in vitro. The incubation time used was 24 hours, as determined in section 3.4.

As shown in Figure 5, the results of the One-way ANOVA statistical analysis show absence of cytotoxicity for concentrations between 2.5 $\mu g.mL^{-1}$ and 35 $\mu g.mL^{-1}$, with cell viability above 70%. The reduction in viability was only observed at the highest concentration of QZ/NC tested. The obtained results demonstrate that the QZ/NC presents compatibility in the specified concentration range. This makes it a potent candidate for use in protocols with biological application and future studies for evaluation of photodynamic activity in models of inflammatory process in vitro.

 doi:10.20944/preprints202405.1323.v1

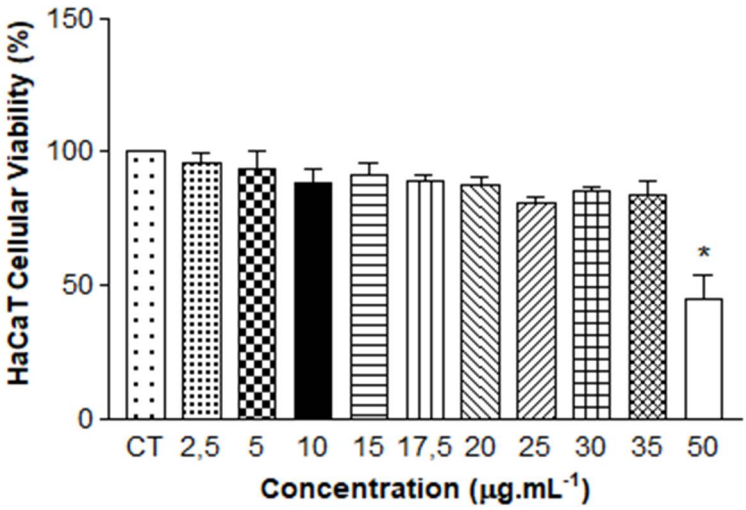

Figure 5. Safety tests from in vitro cytotoxicity assay of QZ/NC on human keratinocyte HaCaT (HaCaT - cell line service) at concentrations of 2.5; 5; 10; 15; 17.5; 20; 25; 30; 35 and 50 µg.mL^{-1} (QZ/NC). Statistical significance was determined using the analysis of variance test One-way ANOVA, at 95% significance level, followed by Tukey post-test for multiple comparisons (*p<0,05).

3.6. Induction of Inflammatory Process in Human Keratinocytes with Application of Photodynamic Therapy and Subsequent Immunoenzymatic Assay

After induction of the inflammatory process, further analyses were performed using the enzyme-linked immunosorbent assay - ELISA, described in 2.9. Cytokines are small proteins secreted in cascade by cells in response to an inflammatory process, influencing interactions and communication between cells. The following pro-inflammatory cytokines were analyzed in this study: Interleukin IL-1β (pro-inflammatory cytokine essential in the inflammatory response and defense of cells, and exacerbates damage in chronic diseases and acute tissue injury [47]; Interleukin IL- 8 (chemokine responsible for the migratory stimulation of neutrophils and other immune cells to the site of inflammation [48], in addition to stimulating the cell proliferation of keratinocytes [48] and monocyte chemotactic protein-1 MCP-1 (responsible for regulating the release of monocytes/macrophages at the site of inflammation [50].

The results obtained are summarized in Figure 6. It is possible to observe the induction of the inflammatory process, where LPS levels were significant compared to the control containing only HaCaT cells, leading to the expression of cytokines IL-1β, IL-8 and MCP1.

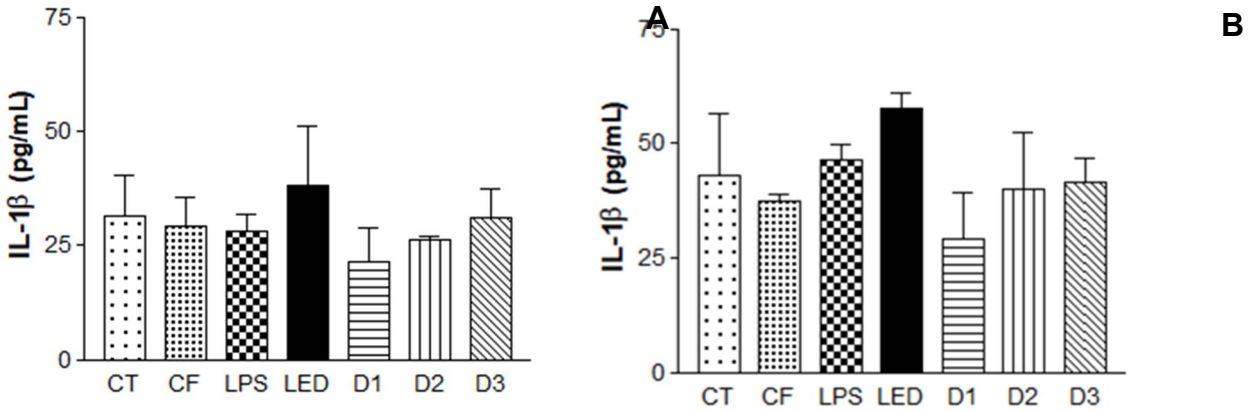

 doi:10.20944/preprints202405.1323.v1

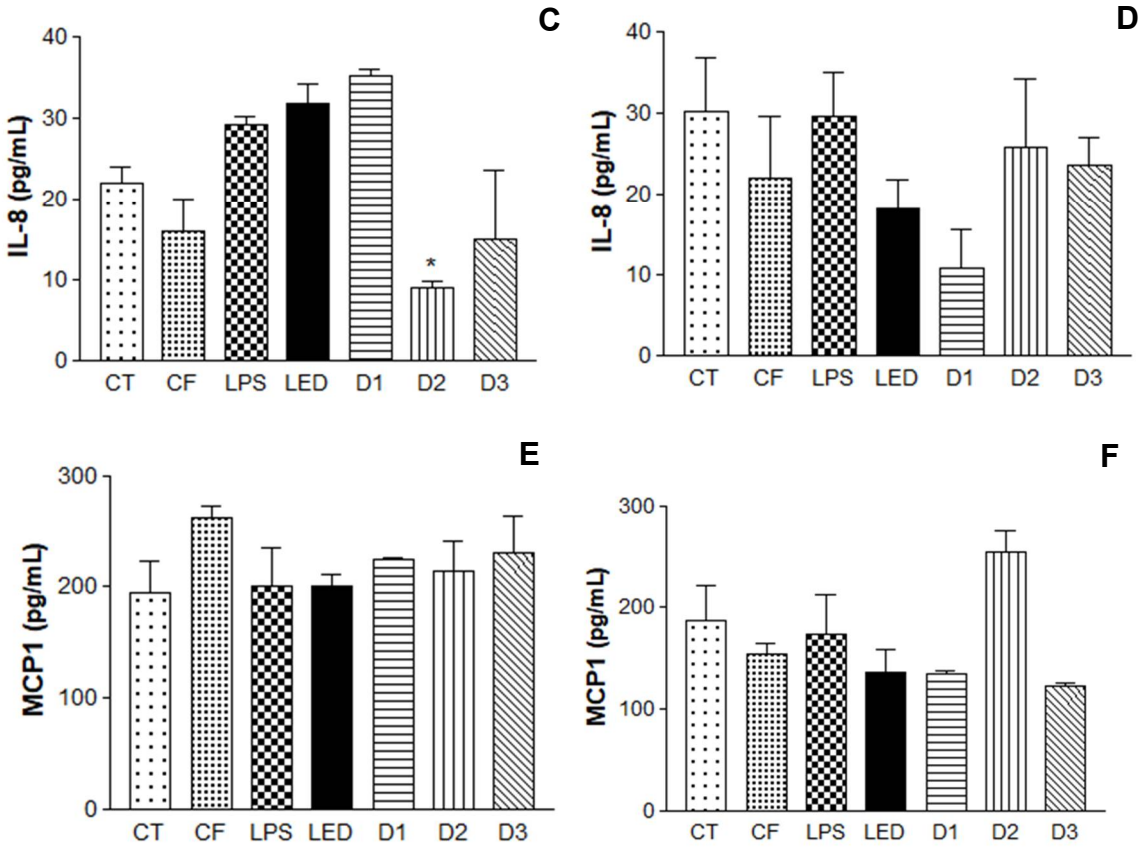

Figure 6. Enzyme-Linked Immunosorbent Assay (ELISA) for the analysis of IL-1β, IL-8 cytokines and macrophages MCP1 in Human Keratinocytes (HaCaT - cell line service) where **A**, **C** and **E**: analysis **6h** after irradiation and **B**, **D** and **F**: analysis **24h** after irradiation, where: CT= Control; LPS = Lipopolysaccharide; LED = irradiation dose of 10 J. cm^{-2}; D1 = QZ/NC irradiation dose of 1.0 $J.cm^{-2}$; D2 = QZ/NC irradiation dose of 5 $J.cm^{-2}$; D3 = QZ/NC irradiation dose of 10 $J.cm^{-2}$; CF= Formulation control (QZ/NC 15µg.mL^{-1}). Statistical significance was determined using the One-way ANOVA analysis of variance test, with a 95% significance level, followed by the Dunnett's post test.

Once the inflammatory process is triggered in vitro, inflammatory mediators initiate the production of cytokines, which play key roles in the inflammatory response [51]. Previous studies have analyzed the action of PDT as a therapeutic method through the production of cytokines, observing an increase in pro-inflammatory cytokines (IL-1β, IL-8, IL-6 and MCP1), highlighting that the action of PDT has three phases: generation of ROS; expression of local endothelial damage and the mechanisms of the disease, so patients who responded to PDT had their levels of pro-inflammatory cytokines increased, as a response to the inflammatory process [52–54]. Also, in comparison with PDT and LED therapy, PDT proved to be more effective in reducing cytokine expression 24 hours after irradiation, when compared to the action of LED alone (therapeutic LED effect) [55,56].

In the analysis of the cytokines IL-1β and IL-8, after 24 hours of irradiation, the formulation had no influence on the level of cytokines, further corroborating the hypothesis that the association of the photosensitizer with the action of the LED is more effective (photodynamic effect). Regarding the energy doses used, the results varied depending on the cytokine analyzed in relation to the time observed. IL-1β, 6 hours after irradiation, showed no statistically significant between the doses analyzed. However, D1 had a considerable reduction in cytokine expression after 24 hours. IL-8, 6h after, D2 and D3 showed significant differences when compared to the control. After 24h, D1 had the most significant difference of the group. MCP1 at 6h after irradiation showed no difference between doses. However, after 24 hours, D1 and D3 showed a reduction in the expression of this cytokine.

The PDT showed greater potential, compared to LED therapy (LED use only) and the QZ/NC formulation applied without any irradiation. Considering the cytokines analyzed above are directly

 doi:10.20944/preprints202405.1323.v1

linked to the inflammatory process of autoimmune and inflammatory diseases, these results show PDT as an effective treatment with potential to be explored in the future.

4. Conclusions

A new therapeutic modality using nanomedicine resources and photodynamic therapy was successfully developed in the field of inflammatory process of skin diseases. The nanomaterials developed presented submicron, and stability in the analysis time, with interesting photophysical properties due to the presence of quinizarin. Spectroscopic studies showed no alterations in the photophysical characteristics of the free and nanoencapsulated photosensitizer. In vitro biological tests showed low toxicity levels, which is a requirement for the application of nanomaterials. The permeation studies in a 3D skin model and cellular uptake showed the permeation of QZ/NC in skin-like models and the intracellular incorporation and internalization of the drug, respectively, enhancing its action in the drug delivery technique. The in vitro inflammatory process was developed, with subsequent application of PDT and immuno-enzymatic analysis, in which it was possible to observe representative effects of PDT when compared to the action of LED and QZ/NC alone, presenting highly favorable results in the use of the model developed for induction of the inflammatory process in vitro and the use of the synthesized nanomaterial, together with PDT, thus representing a possible new therapeutic approach.

Author Contributions: Stéphanie R. do Amaral: Writing - original draft, Methodology, Formal analysis, Validation, Data curation, Statistical analysis. Camila F. Amantino: Methodology, Writing review & editing. Aleksandar Atanasov: Methodology, Validation, Writing review & editing. Stefanie Souza: Methodology, Statistical analysis, Writing review & editing. Richard Moakes: Methodology. Sônia M. Oliani: Writing review & editing. Liam M. Grover: Writing review & editing. Fernando L. Primo: Writing - review & editing, Funding acquisition, Writing - original draft, Project administration, Resources, Formal analysis, Supervisor.

Acknowledgments: The authors acknowledge the Brazilian agencies, National Council for Scientific and Technological Development (CNPq) grants (S.R.A.) and Universal Project # 404416/2021-7 (CNPq) grants (F.L.P.) for their financial support. Prof. Dr. Rondinelli Donizetti Herculano and M.D. Mateus Scontri at Department of Bioprocess Engineering and Biotechnology of School of Pharmaceutical Sciences UNESP-Araraquara/SP for AFM analysis. Prof. Dr. Marlus Chorilli at Department of Department of Pharmaceuticals and Medicines of School of Pharmaceutical Sciences UNESP-Araraquara/SP for DLS equipment support and Profa. Dra. Carla Raquel Fontana Mendonça at Department of Clinical Analyses of School of Pharmaceutical Sciences UNESP-Araraquara/SP for Biotable LED support; and CAPES Print Project to UoB procees n°88887.839000/2023-00 – UNESP training mission (S.R.A).

Conflicts of Interest: The authors declare no conflict of interest.

References

1. Kolarsick, Paul AJ, Maria Ann Kolarsick, and Carolyn Goodwin. "Anatomy and physiology of the skin." Journal of the Dermatology Nurses' Association 3.4 (2011): 203-213. https://doi.org/10.1097/JDN.0b013e3182274a98
2. Lee, Te-An, et al. "Critical roles of irradiance in the regulation of UVB-induced inflammasome activation and skin inflammation in human skin keratinocytes." Journal of Photochemistry and Photobiology B: Biology 226 (2022): 112373. https://doi.org/10.1016/j.jphotobiol.2021.112373
3. Sim, Woo-Jin, et al. "Particulate matter-induced skin inflammation is suppressed by polyphenol-enriched dietary supplement via inhibition of the AhR/ARNT signaling pathway." Journal of Functional Foods 106 (2023): 105593. https://doi.org/10.1016/j.jff.2023.105593
4. Klicznik, M. M., et al. "Taking the lead–how keratinocytes orchestrate skin T cell immunity." Immunology letters 200 (2018): 43-51. https://doi.org/10.1016/j.imlet.2018.06.009
5. Gustafsson, Anna, et al. "Effect of IFN-γ on the kynurenine/tryptophan ratio in monolayer-cultured keratinocytes and a 3D reconstructed human epidermis model." Journal of Dermatological Science 99.3 (2020): 177-184. https://doi.org/10.1016/j.jdermsci.2020.07.005
6. Devos, Michael, et al. "Keratinocyte expression of A20/TNFAIP3 controls skin inflammation associated with atopic dermatitis and psoriasis." Journal of Investigative Dermatology 139.1 (2019): 135-145. https://doi.org/10.1016/j.jid.2018.06.191
7. Zhang, Yiya, et al. "Nav1. 8 in keratinocytes contributes to ROS-mediated inflammation in inflammatory skin diseases." Redox Biology 55 (2022): 102427. https://doi.org/10.1016/j.redox.2022.102427

 doi:10.20944/preprints202405.1323.v1

8. Hari, Gangadhar, Anoop Kishore, and Karkala Sreedhara Ranganath Pai. "Treatments for psoriasis: A journey from classical to advanced therapies. How far have we reached?." European Journal of Pharmacology (2022): 929, 175147. https://doi.org/10.1016/j.ejphar.2022.175147
9. Jin, Yiguang, et al. "Nanostructures of an amphiphilic zinc phthalocyanine polymer conjugate for photodynamic therapy of psoriasis." Colloids and Surfaces B: Biointerfaces (2015): 128, 405-409. https://doi.org/10.1016/j.colsurfb.2015.02.038
10. Hazari, Sahim Aziz, et al. "An overview of topical lipid-based and polymer-based nanocarriers for treatment of psoriasis." International Journal of Pharmaceutics (2023): 122938. https://doi.org/10.1016/j.ijpharm.2023.122938
11. Aleem, Daniyal, and Hassaan Tohid. "Pro-inflammatory cytokines, biomarkers, genetics and the immune system: a mechanistic approach of depression and psoriasis." Revista Colombiana de Psiquiatría (2018): 47, 177-186. https://doi.org/10.1016/j.rcp.2017.03.002
12. Yang, Yixi, et al. "Khasianine ameliorates psoriasis-like skin inflammation and represses TNF-α/NF-κB axis mediated transactivation of IL-17A and IL-33 in keratinocytes." Journal of Ethnopharmacology 292 (2022): 115124. https://doi.org/10.1016/j.jep.2022.115124
13. Mascarenhas-Melo, Filipa, et al. "Nanocarriers for the topical treatment of psoriasis-pathophysiology, conventional treatments, nanotechnology, regulatory and toxicology." European Journal of Pharmaceutics and Biopharmaceutics (2022): 176, 95-107. https://doi.org/10.1016/j.ejpb.2022.05.012
14. Tambe, Varunesh Sanjay, Avni Nautiyal, and Sarika Wairkar. "Topical lipid nanocarriers for management of psoriasis-an overview." Journal of Drug Delivery Science and Technology (2021): 64, 102671. https://doi.org/10.1016/j.jddst.2021.102671
15. Wang, Zixuan, et al. "Application of photodynamic therapy in cancer: challenges and advancements." Biocell (2021): 45, 489. https://doi.org/10.32604/biocell.2021.014439
16. Makuch, Sebastian, et al. "An Update on Photodynamic Therapy of Psoriasis—Current Strategies and Nanotechnology as a Future Perspective." International journal of molecular sciences 23.17 (2022): 9845. https://doi.org/10.3390/ijms23179845
17. Kwiatkowski, Stanisław, et al. "Photodynamic therapy–mechanisms, photosensitizers and combinations." Biomedicine & pharmacotherapy (2018): 106, 1098-1107. https://doi.org/10.1016/j.biopha.2018.07.049
18. Agazzi, Maximiliano L., et al. "BODIPYs in antitumoral and antimicrobial photodynamic therapy: An integrating review." Journal of Photochemistry and Photobiology C: Photochemistry Reviews (2019): 40, 21-48. https://doi.org/10.1016/j.jphotochemrev.2019.04.001
19. Ree, Jin, et al. "Quinizarin suppresses the differentiation of adipocytes and lipogenesis in vitro and in vivo via down-regulation of C/EBP-beta/SREBP pathway." Life Sciences (2021): 287, 120131. https://doi.org/10.1016/j.lfs.2021.120131
20. Singh, Amritpal. Herbal drugs as therapeutic agents. CRC Press, 2014.
21. Malik, Enas M., and Christa E. Müller. "Anthraquinones as pharmacological tools and drugs." Medicinal research reviews (2016): 36, 705-748. https://doi.org/10.1002/med.21391
22. Vázquez, MF Barrera, et al. "Experimental measurement and modeling of quinizarin solubility in pressurized hot water." The Journal of Supercritical Fluids (2017): 125, 1-11. https://doi.org/10.1016/j.supflu.2016.12.020
23. Quinti, Luisa, et al. "A study of the strongly fluorescent species formed by the interaction of the dye 1, 4-dihydroxyanthraquinone (quinizarin) with Al (III)." Journal of Photochemistry and Photobiology A: Chemistry (2003): 155, 79-91. https://doi.org/10.1016/S1010-6030(02)00360-X
24. Hu, Xiufang, et al. "Design and synthesis of various quinizarin derivatives as potential anticancer agents in acute T lymphoblastic leukemia." Bioorganic & Medicinal Chemistry (2019): 27, 1362-1369. https://doi.org/10.1016/j.bmc.2019.02.041
25. Toader, Ana Maria, and Mirela Enache. "QUINIZARIN INTERACTION WITH BILE SALTS MICELLES AS BIOMIMETIC MODEL MEMBRANES." Revue Roumaine de Chimie (2021): 66, 75-80. https://doi.org/10.33224/rrch.2021.66.1.08
26. Díaz-Muñoz, Manuel D., and Martin Turner. "Uncovering the role of RNA-binding proteins in gene expression in the immune system." Frontiers in immunology (2018): 9, 1094. https://doi.org/10.3389/fimmu.2018.01094
27. Amantino, Camila F., et al. "Anthraquinone encapsulation into polymeric nanocapsules as a new drug from biotechnological origin designed for photodynamic therapy." Photodiagnosis and Photodynamic Therapy (2020): 31, 101815. https://doi.org/10.1016/j.pdpdt.2020.101815
28. Abed, Elham Maghareh, et al. "Use of nanotechnology in the diagnosis and treatment of coronavirus." Journal of Current Biomedical Reports (2021): 2, 2717-1906
29. Neto, Serafim Florentino, et al. "α-amyrin-loaded nanocapsules produce selective cytotoxic activity in leukemic cells." Biomedicine & Pharmacotherapy (2021): 139, 111656. https://doi.org/10.1016/j.biopha.2021.111656

 doi:10.20944/preprints202405.1323.v1

30. Jain, Pooja, Himanshu Kathuria, and Nileshkumar Dubey. "Advances in 3D bioprinting of tissues/organs for regenerative medicine and in-vitro models." Biomaterials 287 (2022): 121639. https://doi.org/10.1016/j.biomaterials.2022.121639
31. Aazmi, Abdellah, et al. "Biofabrication methods for reconstructing extracellular matrix mimetics." Bioactive Materials 31 (2024): 475-496. https://doi.org/10.1016/j.bioactmat.2023.08.018
32. Banerjee, Dishary, et al. "Strategies for 3D bioprinting of spheroids: A comprehensive review." Biomaterials (2022): 121881. https://doi.org/10.1016/j.biomaterials.2022.121881
33. Moakes, Richard JA, et al. "A suspended layer additive manufacturing approach to the bioprinting of tri-layered skin equivalents." APL bioengineering 5.4 (2021). https://doi.org/10.1063/5.0061361
34. Siqueira-Moura, Marigilson P., et al. "Development, characterization, and photocytotoxicity assessment on human mel-anoma of chloroaluminum phthalocyanine nanocapsules." Materials Science and Engineering: C (2013): 33, 1744-1752. https://doi.org/10.1016/j.msec.2012.12.088
35. Cardoso, Luana Pereira, et al. "Piperine Reduces Neoplastic Progression in Cervical Cancer Cells by Downregulating the Cyclooxygenase 2 Pathway." Pharmaceuticals (2023): 16, 103. https://doi.org/10.3390/ph16010103
36. Daneshfar, Reza, Siavash Ashoori, and Bahram Soltani Soulgani. "Interaction of electrolyzed nanomaterials with sandstone and carbonate rock: Experimental study and DLVO theory approach." Geoenergy Science and Engineering 230 (2023): 212218. https://doi.org/10.1016/j.geoen.2023.212218
37. Varenne, F., et al. "Towards quality assessed characterization of nanomaterial: Transfer of validated protocols for size measurement by dynamic light scattering and evaluation of zeta potential by electrophoretic light scattering." International Journal of Pharmaceutics (2017): 528, 299-311. https://doi.org/10.1016/j.ijpharm.2017.06.006.
38. Souto, Eliana B., et al. "Physicochemical and biopharmaceutical aspects influencing skin permeation and role of SLN and NLC for skin drug delivery." Heliyon (2022): 8, e08938. https://doi.org/10.1016/j.heliyon.2022.e08938
39. Ghasemiyeh, Parisa, and Soliman Mohammadi-Samani. "Potential of nanoparticles as permeation enhancers and targeted delivery options for skin: Advantages and disadvantages." Drug design, development and therapy (2020): 3271-3289. https://doi.org/10.2147/DDDT.S264648
40. Logue, Brian A., and Erica Manandhar. "Percent residual accuracy for quantifying goodness-of-fit of linear calibration curves." Talanta 189 (2018): 527-533. https://doi.org/10.1016/j.talanta.2018.07.046
41. Pan, Zhao, et al. "A simple and quick method to detect adulterated sesame oil using 3D fluorescence spectra." Spectrochimica Acta Part A: Molecular and Biomolecular Spectroscopy 245 (2021): 118948. https://doi.org/10.1016/j.saa.2020.118948.
42. Gobo, Graciely Gomides, et al. "Novel quinizarin spray-dried nanoparticles for treating melanoma with photodynamic therapy." Materials Today Communications 33 (2022): 104882. https://doi.org/10.1016/j.mtcomm.2022.104882
43. Huerta-García, Elizabeth, et al. "Internalization of titanium dioxide nanoparticles by glial cells is given at short times and is mainly mediated by actin reorganization-dependent endocytosis." Neurotoxicology (2015): 51, 27-37. https://doi.org/10.1016/j.neuro.2015.08.013
44. Batheja, Priya, et al. "Topical drug delivery by a polymeric nanosphere gel: formulation optimization and in vitro and in vivo skin distribution studies." Journal of controlled release 149.2 (2011): 159-167. https://doi.org/10.1016/j.jconrel.2010.10.005
45. Barbosa, Ana Isabel, Sofia A. Costa Lima, and Salette Reis. "Development of methotrexate loaded fucoidan/chitosan nanoparticles with anti-inflammatory potential and enhanced skin permeation." International journal of biological macromolecules 124 (2019): 1115-1122. https://doi.org/10.1016/j.ijbiomac.2018.12.014
46. Poumay, Yves, and Alain Coquette. "Modelling the human epidermis in vitro: tools for basic and applied research." Archives of dermatological research 298 (2007): 361-369. https://doi.org/10.1007/s00403-006-0709-6
47. Lopez-Castejon, Gloria, and David Brough. "Understanding the mechanism of IL-1β secretion." Cytokine & growth factor reviews (2011): 22, 189-195. https://doi.org/10.1016/j.cytogfr.2011.10.001
48. El Ayadi, Amina, David N. Herndon, and Celeste C. Finnerty. "Biomarkers in burn patient care." Total burn care. Elsevier, (2018): 5, 232-235. https://doi.org/10.1016/B978-0-323-47661-4.00021-6
49. Gillitzer, Reinhard, et al. "Upper keratinocytes of psoriatic skin lesions express high levels of NAP-1/IL-8 mRNA in situ." Journal of investigative dermatology (1991): 97, 73-79. https://doi.org/10.1111/1523-1747.ep12478128
50. Deshmane, Satish L., et al. "Monocyte chemoattractant protein-1 (MCP-1): an overview." Journal of interferon & cytokine research (2009): 29, 313-326. https://doi.org/10.1089/jir.2008.0027
51. Yang, Wenxian, et al. "Delicate regulation of IL-1β-mediated inflammation by cyclophilin A." Cell reports (2022): 38, 110513. https://doi.org/10.1016/j.celrep.2022.110513

 doi:10.20944/preprints202405.1323.v1

52. Muñoz-Mata, Lenin Saúl, et al. "Photodynamic therapy stimulates IL-6 and IL-8 in responding patients with HPV infection associated or not with LSIL." Journal of Photochemistry and Photobiology (2022): 11, 100137. https://doi.org/10.1016/j.jpap.2022.100137
53. Suárez-Valladares, María Jesús, et al. "Inflammatory response and cytokine levels induced by intralesional photodynamic therapy and 630-nm laser in a case series of basal cell carcinoma." Journal of the American Academy of Dermatology (2018): 79, 580-582. https://doi.org/10.1016/j.jaad.2018.02.060
54. Lembo, Serena, et al. "MCP-1 in psoriatic patients: effect of biological therapy." Journal of dermatological treatment (2014): 25, 83-86. https://doi.org/10.3109/09546634.2013.782091
55. Akram, Zohaib, et al. "Effect of photodynamic therapy and laser alone as adjunct to scaling and root planing on gingival crevicular fluid inflammatory proteins in periodontal disease: a systematic review." Photodiagnosis and photodynamic therapy (2016): 16, 142-153. https://doi.org/10.1016/j.pdpdt.2016.09.004
56. Klaus, Federica, et al. "Chemokine MCP1 is associated with cognitive flexibility in schizophrenia: A preliminary analysis." Journal of psychiatric research (2021): 138, 139-145. https://doi.org/10.1016/j.jpsychires.2021.04.007